C. R. Physique 15 (2014) 640–647

Contents lists available at ScienceDirect

Comptes Rendus Physique

www.sciencedirect.com

Emergent phenomena in actinides / Phénomènes émergents dans les actinides

Role of electron correlation effects in δ-Pu and "115"-Pu-based unconventional superconductors

Rôle des effets de corrélation électronique dans δ-Pu et dans les supraconducteurs non conventionnels de la famille Pu-115

Alexander B. Shick *, Jindrich Kolorenč

Institute of Physics, ASCR, Na Slovance 2, CZ-18221 Prague, Czech Republic

ARTICLE INFO

Article history:
Available online 17 July 2014

Keywords:
Electronic structure
Strong electron correlations
Photoemission
Unconventional superconductivity

Mots-clés :
Structure électronique
Corrélations électroniques fortes
Photoémission
Supraconductivité non conventionnelle

ABSTRACT

Electronic structure calculations combining the local density approximation with an exact diagonalization of the Anderson impurity model show intermediate $5f^5$–$5f^6$-valence ground state and delocalization of the $5f^5$ multiplet of the Pu atom 5f-shell in $PuCoGa_5$, and δ-Pu. The 5f-local magnetic moment is compensated by a moment formed in the surrounding cloud of conduction electrons. For $PuCoGa_5$ and δ-Pu the compensation is complete and the Anderson impurity ground state is a singlet. This can be important for analyses of the superconducting pairing mechanism in $PuCoGa_5$. It is likely that in $PuCoGa_5$ unconventional *d*-wave superconductivity is mediated by the 5f-states valence fluctuations, rather than antiferromagnetic fluctuations.

RÉSUMÉ

Les méthodes de calcul des structures électroniques qui combinent l'approximation de densité locale avec une diagonalisation exacte du modèle d'impureté d'Anderson prévoyaient, pour δ-Pu et pour $PuCoGa_5$, un état fondamental de valence intermédiaire $5f^5$–$5f^6$, ainsi qu'une délocalisation de la couche électronique 5f du Pu. Le moment magnétique local 5f est compensé par un moment formé dans le milieu des électrons de conduction. Pour $PuCoGa_5$ et δ-Pu, cette compensation est complète et l'état fondamental de l'impureté d'Anderson est un singulet non magnétique. Ce résultat peut avoir des conséquences importantes sur l'analyse des mécanismes de couplage de Cooper dans $PuCoGa_5$. Il est possible que la supraconductivité non conventionnelle de symétrie *d* dans $PuCoGa_5$ soit véhiculée par des fluctuations de valence des états 5f plutôt que par des fluctuations magnétiques.

* Corresponding author.

http://dx.doi.org/10.1016/j.crhy.2014.06.006
1631-0705/

1. Introduction

In order to realize the full potential of nuclear power while minimizing associated risks for society and environment, there is a need to solve many problems in the material science of actinides, by advancing the comprehension of their physical and chemical properties at the microscopic level.

Theoretical modeling of the electronic, structural, and magnetic character of heavy-actinide materials and their 5f-manifold states is very difficult. The standard electronic structure tools of solid state physics, based on density functional theory (DFT), cannot indeed be taken as a reliable vehicle to describe actinides and their compounds. The unique physical properties of these heavy elements originate from the character of the 5f electrons, at the verge of a localization–delocalization instability, and require many new body tools and concepts.

Here, we present some attempts to provide a material-specific theory by including the rotationally invariant multi-orbital Coulomb interaction in the relativistic DFT approach, taking into account spin–orbit coupling. In particular, we describe the results of correlated band theoretical calculations such as (i) the static local (spin) density plus Coulomb U (LDA + U) and (ii) the dynamical LDA + Hubbard-I (LDA + HIA) and LDA + Exact Diagonalization (LDA + ED) approximations, implemented in the full-potential linearized augmented plane wave basis (FP-LAPW).

In what follows, we focus on Pu-based metallic materials where the relativistic effects play a very essential role for the band structure and interaction components of the model. First, we discuss the applications of LDA + U, LDA + HIA, and LDA + ED to the electronic structure and photoemission of δ-Pu, showing that multiplet transitions need to be incorporated into the electronic structure calculations in order to reproduce experimental data. Next, we consider the electron correlation effects in the Pu-115 family ($PuCoGa_5$ and related materials), and compare them with those in elemental plutonium.

$PuCoGa_5$ exhibits superconductivity below a critical temperature of 18.5 K, which is one order of magnitude higher than for typical heavy-fermion compounds. The electron-pairing mechanism in the Pu-115 family is still obscure, and is the subject of heated debates. It is suggested that fluctuations of the residual magnetic moment as well as valence fluctuations are key ingredients of the superconductivity in these compounds.

2. Non-magnetic ground state of δ-Pu

It is commonly accepted that 5f-electrons in light actinides form rather broad conduction bands, whereas for the heavy actinides the 5f states are atomic-like. The atomic volume is an important indicator of the nature of the 5f-electronic states. Withdrawing the 5f states from the bonding and confining them in the ionic core leads to a significant volume expansion. On the plot of atomic volumes of elements, Pu (α) represents a continuation of light actinides, with the decreasing branch resembling the parabolic behavior of transition metals. On the other hand, heavy actinides, starting with Am ($Z = 95$), display a higher volume and a contraction with increasing the atomic number similar to the one displayed by lanthanides. Johansson [1] described this situation as a "Mott transition in the 5f-electron subsystem" taking place between Pu and Am when moving along the Periodic Table.

Plutonium exhibits six allotropic modifications at ambient pressure, some of them of very low symmetry (monoclinic). There is little doubt that this anomalous behaviour is related to the 5f electronic states, being at the border between the localized, non-bonding, behaviour and the bonding situation of electronic bands. δ-Pu, with a volume intermediate between those of α-Pu and Am, represents therefore the cross-over regime, where the electron–electron correlations play a prominent role. Katsnelson et al. [2] linked the broadening of the 5f band to the "atomic collapse" characterizing the transformation from the high-temperature expanded and the low-temperature compressed phases of Pu.

Ab-initio electron energy calculations based on Density Functional Theory (DFT) in the Local Density (LDA) or Generalized Gradient (GGA) approximations account generally well for basic properties of metallic systems. Numerous variants of this successful paradigm were applied to Pu phases. The most conspicuous failure is the case of δ-Pu calculations, which inevitably lead to magnetic ordering. The fact that the lattice expansion due to magnetism yields approximately correct values of the volume, and the intransigence on magnetic order implied by DFT theory, both within LDA and GGA approximations, led to speculations about magnetic ordering of δ-Pu. But experimental findings (magnetic susceptibility has a character of weak Pauli paramagnet—a paramagnetic state is also evidenced—, ^{69}Ga NMR results [3], and neutron scattering [4]) contradict this conclusion.

The challenging question about the absence of magnetism in the δ-Pu phase cannot be answered by DFT theory. At first, this problem was addressed making use of a well-known L(S)DA + U method. Generally, LDA + U calculations account for the on-site correlations between the f electrons in a more realistic way than LSDA calculations. First applied to δ-Pu by Savrasov and Kotliar [5], it also leads to a magnetic solution. Contrary to [5], we applied to δ-Pu a different version of the LDA + U method, namely one that is based on the original LDA + U total energy functional of Ref. [6]. We show that when the LDA + U of Ref. [6] is reformulated in a spin and orbital rotationally invariant form, it yields a basically non-magnetic δ-Pu with $S_z \to 0$ and $L_z \to 0$ [7].

The correlated band theory L(S)DA + U method consists of the local spin-density approximation (LSDA) augmented by a correcting energy of a multiband Hubbard-type E_{ee} and a "double-counting" subtraction term E_{dc}, which accounts approximately for an electron–electron interaction energy already included in LSDA. The form of "Coulomb-U" correction to the LDA is not uniquely defined, and the most commonly used is the version of LDA + U total energy functional in a

Table 1
Ground-state spin M_S, orbital M_L, and total $M_J = M_S + M_L$ magnetic moments (in μ_B) in δ-Pu calculated for an antiferromagnetic configuration at the experimental lattice parameter $a = 8.760$ a.u. using LSDA, and AMF–LSDA + U ($U = 4$ eV) models. Also given are the equilibrium volume V_{eq} (in (a.u.)^3) and the bulk modulus B.

Model	M_S	M_L	M_J	V_{eq}	B (kbar)
LSDA	4.357	−2.020	2.337	13 6.8	761
AMF LSDA + U	∼ 0	∼ 0	∼ 0	181.5	314
Experiment	N/A	N/A	0	168	299

so-called "fully localized" limit (FLL) [5], in which the double-counting term E_{dc} is taken to satisfy an atomic-like limit of the LDA total energy.

Historically, the first LDA + U functional is often called as an "around-mean-field" (AMF) limit of the LDA + U. In this AMF–LDA + U limit [6,8] the interaction energy takes the form:

$$E_{ee}^{AMF} = \frac{1}{2} \sum_{\gamma_1,\gamma_2,\gamma_3,\gamma_4} \delta n_{\gamma_1,\gamma_2} \big[\langle \gamma_1, \gamma_3 | V^{ee} | \gamma_2, \gamma_4 \rangle - \langle \gamma_1, \gamma_3 | V^{ee} | \gamma_4, \gamma_2 \rangle \big] \delta n_{\gamma_3,\gamma_4}, \tag{1}$$

where V^{ee} is an effective on-site "Coulomb-U" interaction. The combined spin-orbital index $\gamma = (m\sigma)$ is composed of the angular m and spin index σ, and

$$\delta n_{\gamma_1,\gamma_2} = n_{\gamma_1,\gamma_2} - n^{\sigma_1} \delta_{\gamma_1,\gamma_2}, \quad n^{\sigma} = \frac{1}{2l+1} \sum_{m=-l}^{l} n_{m\sigma,m\sigma}, \tag{2}$$

where n_{γ_1,γ_2} is the on-site f-occupation matrix in the spin-orbital space that has to be defined with respect to the chosen localized orbital basis set, and n^{σ} is an average spin-orbital occupation.

We note that the essential feature of Eq. (1) is the presence of spin-off-diagonal elements of the on-site occupation matrix $n_{\gamma_1\gamma_2} \equiv n_{m_1\sigma_1,m_2\sigma_2}$, which are in general non-zero in the presence of spin–orbit coupling (SOC).

Spin M_S, orbital M_L, and total M_J magnetic moments calculated for the Pu atom within the LSDA (see Table 1) are in a very good agreement with previous LSDA calculations. The total f-state occupation $n_f = 5.06$ corresponds to the $5f^5$ state. We performed the AMF–LDA + U calculations starting from the LSDA values of charge and spin densities, and on-site spin and orbital occupations, using $U = 4$ eV and an exchange interaction $J = 0.7$ eV, which are in the range of the commonly accepted values for Pu [5]. Without any constraint, the calculations converged to an almost zero magnetic moment, with remaining M_S and $|M_L|$ less than 0.01 μ_B. We also performed calculations starting from a different FLL–LDA + U antiferromagnetic ground state and obtained essentially the same results. One can then conclude that the AMF–LDA + U yields a fundamentally non-magnetic δ-Pu, in accordance with experimental observations. Importantly, the 5f occupation n_f is increased substantially, from $n_f \approx 5$ in LSDA and FLL–LDA + U to $n_f = 5.44$ (see Table 1), meaning that there is a substantial deviation from the $5f^5$ ionic state. We mention that AMF–LDA + U yields $V_{eq} = 181.5$ eV and $B = 314$ kbar, values that are in a very good agreement with experimental data.

The dependence on the value of Coulomb-U of the spin (M_S), orbital (M_L), and total (M_J) moments calculated within the AMF–LDA + U is as follows: for small values of U ($\approx J$), δ-Pu is magnetic with sizeable M_S and M_L moments that almost cancel each other. As the U value is increased to 1.5 eV, the local moments M_S and M_L disappear and δ-Pu is non-magnetic for realistic values of the Coulomb-U (from 3 to 5 eV).

An important criterion for the assessment of results of electronic structure calculations is given by electron spectroscopies. Although some techniques, such as Bremsstrahlung Isochromate Spectroscopy (BIS), have not yet been applied to Pu, experiments have been performed using high-resolution Ultraviolet Photoelectron Spectroscopy (UPS), mapping the electronic structure down to about 10 eV below E_F, and X-ray photoelectron spectroscopy (XPS) [9,10], which gives information on the screening of the deep core-hole by conduction electrons.

Valence-band spectra of δ-Pu and a handful of other Pu-based systems studied so far exhibit invariably three narrow features, one at E_F or in its close vicinity, the other two at 0.5 and 0.85 eV below E_F, which are called A, B, and C, respectively. Valence-band photoelectron spectra reflect to some extent the density of occupied states in the ground state (DOS). A comparison with the bulk experimental UPS [9,10] (see Fig. 1(a)) shows that LDA + U places the 5f manifold approximately 0.9 eV below the Fermi energy (E_F), in accordance with the experimental C peak position, while it does not resolve correctly the experimental features A and B at the E_F edge.

In order to fix this deficiency, we extend the LDA + U procedure described above towards the DMFT to account for the multiplet transitions that are necessary for a correct description of photoemission excitation spectra. We use the multiorbital HIA, which is suitable for incorporating the multiplet transitions in the electronic structure, as it is explicitly based on the exact diagonalization of an isolated atomic-like f-shell.

We construct the multi-orbital Anderson impurity Hamiltonian [11],

$$H_{imp} = \sum_{\substack{kmm' \\ \sigma\sigma'}} [\epsilon^k]_{mm'}^{\sigma\ \sigma'} b_{km\sigma}^{\dagger} b_{km'\sigma'} + \sum_{m\sigma} \epsilon_f f_{m\sigma}^{\dagger} f_{m\sigma}$$

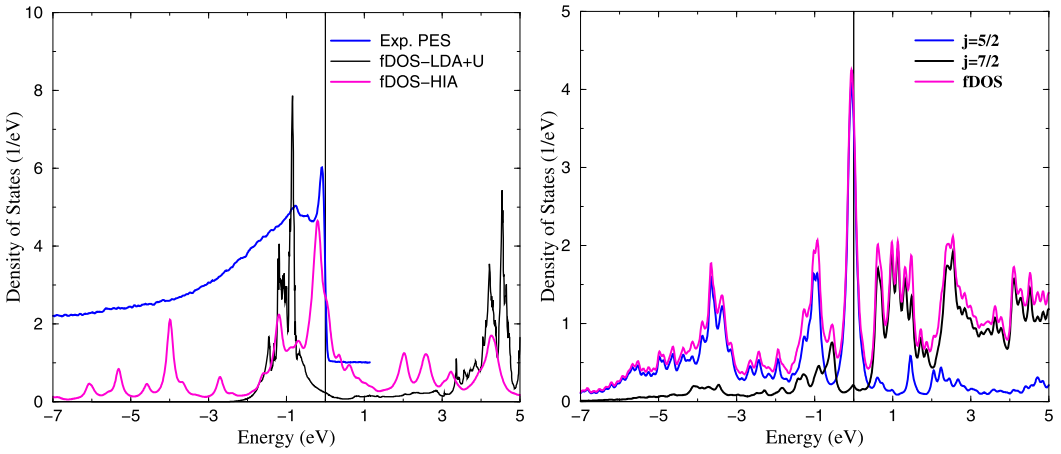

Fig. 1. (Color online.) The δ-Pu fDOS from AMF–LDA + U and LDA + HIA calculations (left panel); total fDOS and $j_{5/2}$, $j_{7/2}$ projected DOS from LDA + ED (right panel). Experimental PES (arb. units) are taken from Ref. [10].

$$+\sum_{mm'\sigma\sigma'}[\xi\mathbf{l}\cdot\mathbf{s}+\Delta_{\mathrm{CF}}]^{\sigma\ \sigma'}_{mm'}f^{\dagger}_{m\sigma}f_{m'\sigma'}$$
$$+\sum_{\substack{kmm'\\ \sigma\sigma'}}\left([V^{k}]^{\sigma\ \sigma'}_{mm'}f^{\dagger}_{m\sigma}b_{km'\sigma'}+\mathrm{h.c.}\right)$$
$$+\frac{1}{2}\sum_{\substack{mm'm''\\ m'''\sigma\sigma'}}U_{mm'm''m'''}f^{\dagger}_{m\sigma}f^{\dagger}_{m'\sigma'}f_{m'''\sigma'}f_{m''\sigma}, \tag{3}$$

where $f^{\dagger}_{m\sigma}$ creates an electron in the 5f shell and $b^{\dagger}_{m\sigma}$ creates an electron in the "bath" that consists of those host-band states that hybridize with the impurity 5f shell. The energy position ϵ_{f} of the impurity level, and the bath energies ϵ^{k} are measured using the chemical potential μ. The parameters ξ and Δ_{CF} specify the strength of the SOC and the size of the crystal field at the impurity. The parameter matrices V^{k} describe the hybridization between the 5f states and the bath orbitals at energy ϵ^{k}.

Once the first and fourth terms are neglected, the Hamiltonian Eq. (3) is reduced to the atomic Hamiltonian H^{at}. This corresponds to the Hubbard-I approximation. Exact diagonalization of $H^{\mathrm{at}}|\nu\rangle = E_{\nu}|\nu\rangle$ is performed to obtain all possible eigenvalues E_{ν} and eigenvectors $|\nu\rangle$. The atomic Green function is calculated as follows:

$$\left[G^{\mathrm{at}}(z)\right]^{\sigma\ \sigma'}_{m_1m_2}(z)=\frac{1}{Z}\sum_{\nu,\mu}\frac{\langle\mu|f_{m_1\sigma}|\nu\rangle\langle\nu|f^{\dagger}_{m_2\sigma'}|\mu\rangle}{z+(E_{\mu}-\mu N_{\mu})-(E_{\nu}-\mu N_{\nu})}$$
$$\times\left[\exp\left(-\beta(E_{\nu}-\mu N_{\nu})\right)+\exp\left(-\beta(E_{\mu}-\mu N_{\mu})\right)\right], \tag{4}$$

and the atomic self-energy is evaluated as:

$$\left[\Sigma_{\mathrm{H}}(z)\right]^{\sigma\ \sigma'}_{mm'}=z\delta_{m_1m_2}\delta_{\sigma\sigma'}-\xi(\mathbf{l}\cdot\mathbf{s})^{\sigma\ \sigma'}_{m_1m_2}-\left[\left(G^{\mathrm{at}}(z)\right)^{-1}\right]^{\sigma\ \sigma'}_{m_1m_2}. \tag{5}$$

The LDA + U Green function is evaluated for the self-consistent LDA + U solution making use of LDA + U eigenvalues and eigenfunctions calculated in the full-potential LAPW basis,

$$G_{+U}(z)=\frac{1}{V_{\mathrm{BZ}}}\int_{\mathrm{BZ}}\mathrm{d}\mathbf{k}\left(z+\mu-H_0(\mathbf{k})-V_{+U}\right)^{-1}. \tag{6}$$

Next, we evaluate the static Weiss field $\mathcal{G}_0(z)$:

$$\mathcal{G}^{0}_{+U}(z)=\left(G^{-1}_{+U}(z)+V_{+U}(z)\right)^{-1}. \tag{7}$$

Then we insert the HIA self-energy, calculated for the same number of correlated electrons as given by LDA + U, into this "bath", and calculate the new Green function

$$G(z)=\left(\left[\mathcal{G}^{+U}_{0}(z)\right]^{-1}+\Delta\epsilon-\Sigma_{\mathrm{H}}(z)\right)^{-1}, \tag{8}$$

where $\Delta\epsilon$ is chosen so as to ensure that $n=\pi^{-1}\,\mathrm{Im}\int^{\mu}\mathrm{d}E\,\mathrm{Tr}[G(E)]$ is equal to a given number of correlated electrons.

In Fig. 1(a) we show the f-projected DOS (fDOS) from AMF–LDA + U together with the spectral density calculated from Eq. (8). For δ-Pu, the AMF–LDA + U fDOS manifold at around -1 eV transforms into a set of multiplet transitions with

high value of spectral density at E_F. There is a good agreement between the HIA calculated fDOS and the experimental PES. While LDA + HIA calculations explain well the experimental PES, the ground state of the f-shell manifold is not a singlet, then the absence of magnetism and temperature-independent magnetic susceptibility remains unexplained.

To proceed further, we extend our procedure, and account for the hybridization between f- and non-f states in the Hamiltonian Eq. (3) [12]. In order to determine the bath parameters V^k and ϵ^k, we assume that LDA represents the non-interacting model. We then associate the LDA Green function $G_{\mathrm{LDA}}(z)$ with the Hamiltonian of Eq. (3) when the coefficients of the Coulomb interaction matrix are set to zero ($U_{mm'm''m'''} = 0$). The hybridization function $\Delta(\epsilon)$ is then estimated as $\Delta(\epsilon) = -\frac{1}{\pi}\,\mathrm{Im}\,\mathrm{Tr}[G^{-1}_{\mathrm{LDA}}(\epsilon + \mathrm{i}\delta)]$ [13]. Also we assume that the most important hybridization is the one occurring in the vicinity of E_F, and that the hybridization matrix is, to a good approximation, diagonal in the $\{j, j_z\}$ representation, so that we only need to specify one bath state (six orbitals) with $\epsilon^{k=1}_{j=5/2}$ and $V^{k=1}_{j=5/2}$, and another bath state (eight orbitals) with $\epsilon^{k=1}_{j=7/2}$ and $V^{k=1}_{j=7/2}$. Then the bath parameters V^k_j, and the bath-state energies ϵ^k_j are chosen to approximately reproduce the LDA 5f-states occupations $n_f^{5/2}$ and $n_f^{7/2}$.

The band Lanczos method [14] is employed to find the lowest-lying eigenstates of the many-body Hamiltonian H_{imp} and to calculate the one-particle Green's function $[G_{\mathrm{imp}}(z)]^{\sigma\ \sigma'}_{mm'}$ in the subspace of the f orbitals at low temperature ($k_B T = 1/500$ eV). The self-energy $[\Sigma(z)]^{\sigma\ \sigma'}_{mm'}$ is then obtained from the inverse of the Green's function matrix $[G_{\mathrm{imp}}]$.

Once the self-energy is known, the local Green's function $G(z)$ for the electrons in the solid is calculated. Then, with the aid of the local Green function $G(z)$, we evaluate the occupation matrix $n_{\gamma_1\gamma_2} = -\frac{1}{\pi}\,\mathrm{Im}\int_{-\infty}^{E_F} \mathrm{d}z\,[G(z)]_{\gamma_1\gamma_2}$. The matrix $n_{\gamma_1\gamma_2}$ is used to construct an effective LDA + U potential V_U, which is inserted into Kohn–Sham-like equations:

$$\left[-\nabla^2 + V_{\mathrm{LDA}}(\mathbf{r}) + V_U + \xi(\mathbf{l}\cdot\mathbf{s})\right]\Phi^b_{\mathbf{k}}(\mathbf{r}) = \epsilon^b_{\mathbf{k}}\Phi^b_{\mathbf{k}}(\mathbf{r}). \tag{9}$$

These equations are iteratively solved until self-consistency over the charge density is reached. In each iteration, a new Weiss field $\mathcal{G}_0(z)$ Eq. (7), and a new value of the 5f-shell occupation are obtained from the solution of Eq. (9). Subsequently, a new self-energy $\Sigma(z)$ corresponding to the updated 5f-shell occupation is constructed. Finally, the next iteration is started by evaluating the new local Green's function, Eq. (8).

In the case of δ-Pu, the hybridized ground state of the impurity is a non-magnetic singlet with all angular moments of the 5f plus bath cluster equal to zero ($S = L = J = 0$). It consists of $\langle n_f\rangle = 5.21$ f states and $\langle n_{\mathrm{bath}}\rangle = 8.79$ bath states. In a pictorial way, we can imagine that the magnetic moment of the 5f shell (for which we get $S_f = 2.11$, $L_f = 4.21$, $J_f = 2.62$) is completely compensated by the moment carried by the electrons in the conduction band. As the value of the 5f magnetic moment fluctuates in time, because of the intermediate valence electronic configuration, this compensation must be understood as dynamical in nature. The 5f-orbital projected DOS is shown in Fig. 1 and is in good agreement with the experimental photoemission spectra. Notice that the multiplets for the atomic f^6 configuration ($f^6 \to f^5$ transition, lying closer to E_F) are better resolved than for the f^5 part of the spectrum ($f^5 \to f^4$ transition).

Analogously to the intermediate valence rare earths [15], the magnetic susceptibility is anticipated to behave as $\chi \sim 1/(T + T_{\mathrm{fc}})$, where the temperature T_{fc} describes fluctuations between 5f and conduction band electron states. T_{fc} corresponds indeed to the broadening of the quasi-particle resonance near E_F due to valence fluctuations [16]. As the ground state of the impurity is a singlet, we estimate T_{fc} using a renormalized perturbation theory of the Anderson model [11], $T_{\mathrm{fc}} = -\frac{\pi^2}{4} Z[\Delta(E_F)/N_f]$, where $[\Delta(E_F)/N_f]$ is the hybridization per orbital at E_F, and Z is a quasi-particle weight ($Z = (\mathrm{Tr}[N(E_F)(1 - \frac{\mathrm{d}\Sigma(\epsilon)}{\mathrm{d}\epsilon})|_{\epsilon=E_F}]/\mathrm{Tr}[N(E_F)])^{-1}$). For δ-Pu, we get $T_{\mathrm{fc}} = 63$ meV (~ 750 K). Since T_{fc} is high, χ remains constant for $T \ll T_{\mathrm{fc}}$, as observed experimentally.

3. Electronic and magnetic character of Pu-atom in $PuCoGa_5$

The intermediate-valence and non-magnetic character of the 5f-shell can play an important role in stabilizing the superconducting state exhibited by $PuCoGa_5$ below a critical temperature T_c of 18.5 K [12]. The unconventional character of superconductivity in this compound [17,3] is now generally accepted, but the microscopic mechanism responsible for electron pairing remains unknown [18]. The d-wave symmetry of the superconducting gap in $PuCoGa_5$ has been proven by point-contact spectroscopy experiments [19], which also provided the first spectroscopic measurements of the gap amplitude and of its temperature dependence.

Keeping in mind a failure of DFT in the case of δ-Pu, it can be expected that LDA/GGA does not provide a reasonable description of the electronic structure for this strongly correlated material. Below, we report electronic structure calculations of $PuCoGa_5$ performed by combining LDA with the exact diagonalization (ED) of a discretized single-impurity Anderson model, making use of the same approach as that described above for the case of δ-Pu [12]. The calculations were carried out assuming a paramagnetic state with crystal structure parameters for $PuCoGa_5$ taken from Ref. [17]. The Slater integrals were chosen as $F_0 = 4.0$ eV, and $F_2 = 7.76$ eV, $F_4 = 5.05$ eV, and $F_6 = 3.07$ eV. They correspond to commonly accepted values for Coulomb $U = 4.0$ eV and exchange $J = 0.64$ eV. The SOC parameter $\xi = 0.29$ eV for $PuCoGa_5$ was determined from LDA calculations. CF effects were found to be negligible and Δ_{CF} was set to zero.

The ground state of the cluster formed by the 5f shell and the bath is a non-magnetic singlet with all angular moments of the 5f-bath cluster equal to zero ($S = L = J = 0$). It consists of $\langle n_f\rangle = 5.30$ f states and $\langle n_{\mathrm{bath}}\rangle = 8.70$ bath states. The magnetic moment of the 5f shell (for which we get $S_f = 2.18$, $L_f = 4.05$, $J_f = 2.43$) is completely compensated by the

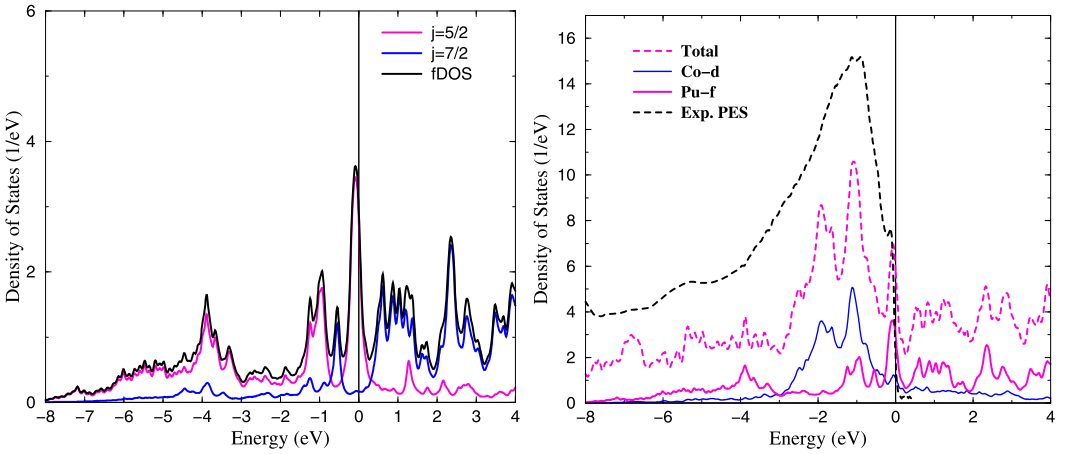

Fig. 2. (Color online.) The $PuCoGa_5$ total fDOS and $j_{5/2}$, $j_{7/2}$ projected DOS from LDA + ED (left panel); the total DOS, Co-dDOS, and Pu-fDOS in comparison with the experimental PES (arb. units) (right panel).

moment carried by the electrons in the conduction band. The 5f-orbital projected DOS is shown in Fig. 2(a). Below Fermi energy, E_F, the DOS exhibits the three-peak structure typical for Pu and for a number of its compounds. As in the case of δ-Pu, it can be noticed that the multiplets for the atomic f^6 configuration ($f^6 \rightarrow f^5$ transition, lying closer to E_F) are better resolved than for the f^5 part of the spectrum ($f^5 \rightarrow f^4$ transition).

The comparison between the DOS and experimental photoemission spectra [20] is shown in Fig. 2(b). The three-peak structure is not resolved in the experiment which shows only the A peak at the Fermi edge. We cannot claim a quantitative agreement between the DOS and the experimental PES. The shape of the total DOS corresponds fairly well to the experimental photoemission spectra. Moreover, the calculations suggest that B- and C-peaks of Pu-5f states are masked by the signal coming mainly from Co-d-states. These are spread over the region from E_F to ≈ 3.5 eV.

The band structure resulting from the solutions of Eq. (9) is shown in Fig. 3 together with the corresponding quasiparticle Fermi surfaces (FS). There are four sheets (I–IV) composing the FS: sheets I and II are fairly three-dimensional and sheets III and IV are two-dimensional. Close similarities are revealed between these sheets and the Fermi surfaces from the previous LDA [21] and AMF–LDA + U calculations.

The role of the electronic structure in determining superconductivity depends on the mechanism. First, we estimate the possibility for electron–phonon-interaction-mediated superconductivity. The Drude plasma energy $\Omega_p = 3.5$ eV is calculated. Now, assuming that the temperature dependence of electrical resistivity is due only to the electron–phonon interaction, we can estimate the electron–phonon coupling λ_{tr} from the Bloch–Grüneisen transport theory, employing an approximate expression [22] $\frac{\Delta\rho}{\Delta T} \approx \frac{8\pi^2}{\hbar\Omega_p^2} k_B \lambda_{tr}$ that relates the electrical resistivity ρ to the electron–phonon coupling strength. Making use of the experimental room-temperature value of ρ, we estimate the electron–phonon coupling λ_{tr} at ≈ 2.5 for $PuCoGa_5$. Inserting $\lambda_{tr} = 2.5$ into the McMillan formula [23] and assuming the Coulomb pseudopotential μ^* to be between 0.0 and 0.2, we obtain an estimate for the superconducting transition temperature T_c in the range 27–39 K, which is not too far from the experimental value $T_c = 18.5$ K. This observation would support the strong electron–phonon coupling mechanism of superconductivity in $PuCoGa_5$. However, recent point-contact spectroscopy measurements [19] are pointing out the d-wave symmetry of the superconducting gap, making the electron–phonon-coupling-mediated superconductivity unlikely.

It has been argued that, in some cases, superconductivity can be driven by Fermi-surface nesting. Nesting, which indicates instability in the FS, can give rise to a spin-density wave or a charge-density wave. The shape of FS shown in Fig. 3 suggests a possibility of either Q_1-nesting between $[\pi, 0, k_z]$ and equivalent k-points of FS-II sheet or Q_2-nesting between the hole-like FS-1 around the $\Gamma = (0, 0, k_z)$ point and electron-like FS-3 around the $M = (\pi, \pi, k_z)$ point. This $q \sim (\pi, \pi, k_z)$ nesting-like feature can lead to a peak in the spin/charge susceptibility, and promote the anti-ferromagnetic or charge fluctuations to develop. The Q_1 nesting instability will promote the $d_{x^2-y^2}$ type of pairing. Recent point-contact spectroscopy measurements [19] are pointing out the d-wave scenario.

The Q_2 nesting would correspond to the so-called $s\pm$ superconductivity, similar to the case of Fe-based superconductors [24]. The strength of the pairing interaction depends on the joint density of states. For Q_2 nesting, it would mean a high value of the product of the DOS near $\Gamma = (0, 0, k_z)$ and $M = (\pi, \pi, k_z)$ points. As follows from the band structure, it is not the case for $PuCoGa_5$. On the other hand, a possibility of Q_1 nesting instability, together with experimental data in [19], support the d-wave scenario. The presence of a 5f local moment dynamically compensated by the surrounding conduction electrons, together with the f^5–f^6 intermediate-valence ground state in $PuCoGa_5$, opens an attractive possibility for valence-fluctuation-mediated superconductivity, in a similar way to the case of heavy-fermion superconductors [25].

To summarize, the LDA + ED calculations show an intermediate $5f^5$–$5f^6$-valence ground state and delocalization of the $5f^5$ multiplet of the Pu atom 5f-shell in $PuCoGa_5$, and δ-Pu. The 5f-local magnetic moment is compensated by a moment formed in the surrounding cloud of conduction electrons. For $PuCoGa_5$ and δ-Pu, the compensation is complete and the

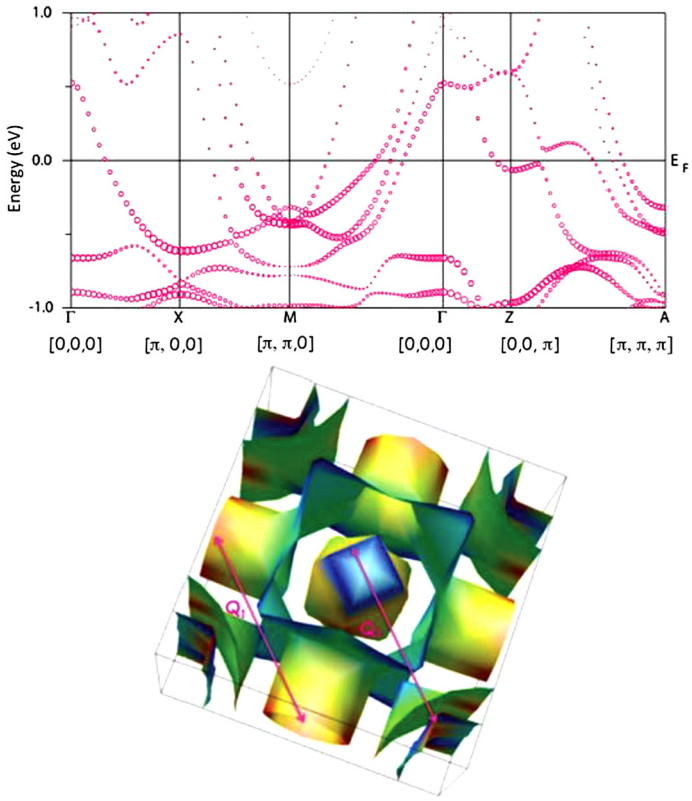

Fig. 3. (Color online.) The $PuCoGa_5$ band structure with f-band character (top); the Fermi surface (bottom) from LDA + ED.

Anderson impurity ground state is a singlet. Our findings can be important for understanding the superconductivity in the "115" family of the materials.

Acknowledgements

We are grateful to R. Caciuffo for helpful discussion during the preparation of this manuscript. The financial support from the Czech Republic Grant No. GACR P204/10/0330 is acknowledged.

References

[1] B. Johansson, Nature of the 5f electrons in the actinide series, Phys. Rev. B 11 (1975) 2740–2743.
[2] M.I. Katsnelson, I.V. Solovyev, A.V. Trefilov, α–δ transition in plutonium as a Mott transition in an f subsystem, JETP Lett. 56 (1992) 272–276.
[3] N.J. Curro, T. Caldwell, E.D. Bauer, L.A. Morales, M.J. Graf, Y. Bang, A.V. Balatsky, J.D. Thompson, J.L. Sarrao, Unconventional superconductivity in $PuCoGa_5$, Nature 434 (2005) 622–625.
[4] J.C. Lashley, A. Lawson, R.J. McQueeney, G.H. Lander, Absence of magnetic moments in plutonium, Phys. Rev. B 72 (2005) 054416.
[5] S.Y. Savrasov, G. Kotliar, Ground state theory of δ-Pu, Phys. Rev. Lett. 84 (2000) 3670–3674.
[6] V.I. Anisimov, J. Zaanen, O.K. Andersen, Band theory and Mott insulators: Hubbard U instead of Stoner I, Phys. Rev. B 44 (1991) 943–954.
[7] A.B. Shick, V. Drchal, L. Havela, Coulomb-U and magnetic-moment collapse in δ-Pu, Europhys. Lett. 69 (2005) 588–594.
[8] M.T. Czyżyk, G.A. Sawatzky, Local-density functional and on-site correlations: the electronic structure of La_2CuO_4 and $LaCuO_3$, Phys. Rev. B 49 (1994) 14211–14228.
[9] T. Gouder, L. Havela, F. Wastin, J. Rebizant, Evidence for the 5f localisation in thin Pu layers, Europhys. Lett. 55 (2001) 705–711.
[10] L. Havela, T. Gouder, F. Wastin, J. Rebizant, Photoelectron spectroscopy study of the 5f localization in Pu, Phys. Rev. B 65 (2002) 235118.
[11] A.C. Hewson, The Kondo Problem to Heavy Fermions, Cambridge University Press, UK, 1993.
[12] A.B. Shick, J. Kolorenc, J. Rusz, P.M. Oppeneer, A.I. Lichtenstein, M.I. Katsnelson, R. Caciuffo, Unified character of correlation effects in unconventional Pu-based superconductors and δ-Pu, Phys. Rev. B 87 (2013) 020505(R).
[13] O. Gunnarsson, O.K. Andersen, O. Jepsen, J. Zaanen, Density-functional calculation of the parameters in the Anderson model: application to Mn in CdTe, Phys. Rev. B 39 (1989) 1708–1722.
[14] J. Kolorenc, A. Poteryaev, A.I. Lichtenstein, Valence-band satellite in ferromagnetic nickel: LDA + DMFT study with exact diagonalization, Phys. Rev. B 85 (2012) 235136.
[15] D.I. Khomskii, The problem of intermediate valency, Sov. Phys. Usp. 22 (1979) 879–903.
[16] C.M. Varma, Y. Yafet, Magnetic susceptibility of mixed-valence rare-earth compounds, Phys. Rev. B 13 (1976) 2950–2954.
[17] J.L. Sarrao, L.A. Morales, J.D. Thompson, B.L. Scott, G.R. Stewart, F. Wastin, J. Rebizant, P. Boulet, E. Colineau, G.H. Lander, Plutonium-based superconductivity with a transition temperature above 18 K, Nature 420 (2002) 297–299.
[18] F. Jutier, G.A. Ummarino, J.-C. Griveau, F. Wastin, E. Colineau, J. Rebizant, N. Magnani, R. Caciuffo, Possible mechanism of superconductivity in $PuCoGa_5$ probed by self-irradiation damage, Phys. Rev. B 77 (2008) 024521.

[19] D. Daghero, M. Tortello, G.A. Ummarino, J.-C. Griveau, E. Colineau, R. Eloirdi, A.B. Shick, J. Kolorenc, A.I. Lichtenstein, R. Caciuffo, Strong-coupling d-wave superconductivity in $PuCoGa_5$ probed by point-contact spectroscopy, Nat. Commun. 3 (2012) 786, http://dx.doi.org/10.1038/ncomms1785.
[20] R. Eloirdi, L. Havela, T. Gouder, A. Shick, J. Rebizant, F. Huber, R. Caciuffo, Photoelectron spectroscopy study of $PuCoGa_5$ thin films, J. Nucl. Mater. 385 (2009) 8–10.
[21] A.B. Shick, V. Janiš, P.M. Oppeneer, Effect of Coulomb correlations on the electronic structure of $PuCoGa_5$, Phys. Rev. Lett. 94 (2005) 016401.
[22] P.B. Allen, Empirical electron–phonon λ values from resistivity of cubic metallic elements, Phys. Rev. B 36 (1987) 2920–2923(R).
[23] W.L. McMillan, Transition temperature of strong-coupled superconductors, Phys. Rev. 167 (1968) 331–344.
[24] I.I. Mazin, D.J. Singh, M.D. Johannes, M.H. Du, Unconventional superconductivity with a sign reversal in the order parameter of $LaFeAsO_{1-x}F_x$, Phys. Rev. Lett. 101 (2008) 057003.
[25] K. Miyake, New trend of superconductivity in strongly correlated electron systems, J. Phys. Condens. Matter 19 (2007) 125201.